Oil Shale, 2009, Vol. 26, No. 3, pp. 399–414
doi: 10.3176/oil.2009.3.05
ISSN 0208-189X

DISSOLUTION RATE OF OIL SHALE THERMOBITUMEN IN DIFFERENT SOLVENTS

I. JOHANNES*, L. TIIKMA, J. SOKOLOVA

Laboratory of Oil Shale and Renewables Research
Tallinn University of Technology
5 Ehitajate Rd., Tallinn 19086, Estonia

Dissolution kinetics of the mix of thermobitumen and oil (TBO) formed at low-temperature pyrolysis of oil shale in autoclaves was studied for the first time. The pyrolysis temperature was varied in the range of 350–370 °C and duration between 3 and 9 hours. The dissolution of TBO obtained was conducted in a thermostated stirred class reactor and evaluated by the increase in optical density of the solutions with time varying temperature (25–60 °C) and solvent type (benzene, toluene, oil shale petrol and ethanol). A mathematical model was deduced for quantitative description of dissolution kinetics by approximation of the process to the first-order parallel dissolution of two fractions. The dissolution rate coefficients for the fractions were estimated, and contribution of their partial optical densities on the current optical density was described under the conditions studied.

Introduction

It is known that at pyrolysis of Estonian oil shale (kukersite) between temperatures 250–350 °C the unwanted plasticization takes place resulting in formation of sticky thermobitumen (TB) and some light fractions. The TB formed is a mix of soluble in organic solvents high-molecular non-volatile intermediate products of kerogen thermal decomposition. At 325–350 °C begins the secondary pyrolysis of TB into oil fractions, gas and semicoke. The physical characteristics and molecular weight of TB depend on its formation conditions [1].

At the present time, formation of TB from oil shale studied intensively in the middle of the last century is of interest again [2–6] in order to perform the isolation of a maximum amount of organic substances from kukersite. Reviews about previous works and the recent experimental results concerning formation of TB from oil shale in Fischer retort and of the mix of TB and oil (TBO) in autoclaves were published in [2] and [3]. The results proved the

* Corresponding author: e-mail *ille.johannes@ttu.ee*

possibility for dissolution about 90% of oil shale organic matter as TBO when the thermal treatment is conducted below the temperature range for coke formation. The yield of the decomposition products in the form of TBO overcomes 1.5 times the oil yield at retorting of kukersite in a laboratory Fischer assay. Besides, the content of hazardous organic matter in semicoke is decreased drastically. The main disadvantage of the thermobituminization process is the comparatively slow formation of TBO (3-5 h) at the low-temperature region required. Kinetics of parallel formation of TB, oil and gas from kukersite, and consecutive formation of gas and coke from TBO or TB was modeled in [4] and [5] for the temperatures range 350–410 °C. It was found [6] that when thermal decomposition of kukersite was conducted in the environment of supercritical water, ethanol or oil shale petrol, the formation of TBO was accelerated whereas the solvents benzene, toluene and sub-critical water had no effect on the decomposition rate in comparison with the process without any solvent. The papers [7] and [8] showed that at liquefaction of the enriched kukersite, kerogen-70, during 4 hours at 360 °C in an autoclave the solvents applied arranged by the yield of liquid products from organic matter as follows, %: water (69.6), *n*-hexane (72.2), benzene (81.5), ethanol (99.0!), diethyl ether (106.3!) and dimethyl ketone (145.7!). At that, the surprisingly high liquid yields obtained with the last three solvents were explained by incorporation of the solvents into TBO.

The liquid and solid products formed at thermal decomposition of oil shale, independently of the solvents applied, were diluted in benzene [3–8] or in the mix of benzene and ethanol [1, 2]. In the next step, the phases were separated by time-consuming Soxhlet extraction with boiling benzene [1–6] or by filtration and washing with benzene at room temperature [7, 8]. Filtration of some gel-like products was travail.

The goal of this work, dissolution rate of TBO formed, has not been studied earlier.

Survey of dissolution models

In [9] an overview about history of dissolution research during the last century was published. According to this report, already in 1897 Noyes and Witny [10] in Massachusetts Institute of Technology proposed the following expression for dissolution rate of solid substances

$$\frac{dC}{dt} = k(S - C), \tag{1}$$

where C was the current concentration at time t, S represented the solubility of the substance, and k was a constant.

Already in the beginning of the 20th century it was shown [1] that the dissolution rate coefficient depended on the stirring rate, temperature, and surface and on the arrangement of the dissolution device. According to

Nernst-Brunner equation [11] dissolution rate expression was advanced basing on the diffusion layer concept as follows:

$$\frac{dC}{dt} = \frac{DA}{Vh}(C_S - C), \tag{2}$$

where D was the diffusion coefficient, A the exposed surface area of the solid, h the thickness of the diffusion layer, and V the volume of the diffusion medium (which was stirred rapidly to insure homogeneity), C_S was the concentration of the dissolved solid in the diffusion layer surrounding the solid.

When a solvent reacts throughout the particle at all times, and the amount of the particles is exhaustible, the dissolution rate can be given in the same form as for a homogeneous reaction where instead of C_S the maximum concentration being attained (the steady state) under the dissolution conditions, $C_{\max}$, is applied.

Up to now, the first order kinetic equation (2) and its integrated form

$$\ln(1-x) = \frac{DA}{Vh}t, \tag{3}$$

where x is C/C_S or $C/C_{\max}$ have been widely applied in dissolution kinetics [12].

When the plot of $C/C_{\max}$ versus t has an asymmetric sigmoidal shape, the semi-empirical "Power Law" model

$$\frac{C}{C_{\max}} = kt^n \tag{4}$$

has been proposed by Peppas [13] where n is a non-physical fit parameter that does not satisfy any physico-chemical model being mathematically derived to-date for phase transformation kinetics.

The generalized integral rate equation of the physico-chemical models is as follows:

$$g(x) = kt, \tag{5}$$

where conversion function $g(x)$ is determined by the process mechanism and should be proportional with time.

A selection from the set of formulas for calculation of $g(x)$ in the most frequently used models for solid-state reactions published in [14] and later applied by several researchers [16–22] are given in Table 1.

The aim of this work was quantitative description of the effect of solvent type on the dissolution rate of TBO. For this aim, the suitable kinetic model was obtained, and the effects of solvent volume and temperature, and of pyrolysis temperature and duration on the total dissolution rate coefficients, k, were elucidated. The individual contribution of the factors of k (D, A, V and h) depending mainly on the substance being dissolved was not discussed in this work handling only TBO.

Table 1. **Integral forms of the conversion function, $g(x)$ [14-22]**

Model type	$g(x)$	Formula No
First-order, Eq. (3)	$-\ln(1-x)$	*I*
n–order	$[1-(1-x)^{1-n}]/(1-n)$	*II*
1D diffusion	x^2	*III*
2D-diffusion	$x+(1-x)\ln(1-x)$	*IV*
3D-diffusion	$[1-(1-x)^{1/3}]^2$	*V*
4D-diffusion	$1-2x/3-(1-x)^{2/3}$	*VI*
Zero-order	x	*VII*
Contracting area	$[1-(1-x)]^{1/2}$	*VIII*
Contracting volume	$[1-(1-x)]^{1/3}$	*IX*
Power law, Eq. (4), $n = 2$	$x^{1/2}$	*X*

Experimental

Materials

The initial air-dry oil shale contained 40% organic matter (kerogen) and 0.57% hygroscopic water. The purity of the solvents applied was of analytical grade, except oil shale petrol. The latter was obtained from the industrial Galoter process [23]. Its density at 20 °C was 0.780 kg/dm^3.

Pyrolysis

The samples of TBO for dissolution tests were prepared by pyrolysis of 1 gram of the initial kukersite in a glass test-tube with inner diameter 10 cm inserted into a 20 cm^3 autoclave. The autoclaves were placed into a muffle oven heated up to various nominal temperatures between 350–370 °C. Pyrolysis duration was varied in the range of 3–9 hours. The gas yield was estimated by the weight loss of the cooled to room temperature and opened autoclaves. The yield of TBO per organic matter was found by subtraction of the yields of gas and solid residue from 100%. The yield of organic solid residue remaining after dissolution was estimated by weight loss at incineration of the acid treated residue. In this way the artifacts concerning overestimated yields of TBO due to incorporation of solvents discussed in [6, 8] were avoided.

The yields of TBO obtained under various conditions are presented in the second column of Tables 2 and 3, and in Fig. 1. The results prove the essential effect of the pyrolysis temperature and duration on the yield of TBO from kukersite known earlier [2–8]. At that, about 30-minute prolongation of the time to reach the maximum yield in comparison with that given earlier [3 and 4] can be explained by an increase of the heating-up time due to additional glass tubes applied for the samples in autoclaves in this work. Noteworthy is the negligible effect of dissolution temperature on the total yield of TBO. The vital effect of the dissolution conditions on the dissolution kinetics will be discussed later below.

Table. 2. **Characteristic constants for TBO dissolution in benzene**

The default conditions: benzene volume per kukersite 100 cm^3/g; dissolution temperature – 60 °C; dilution factor of the solutions before estimation of their optical density – 10; wave length – 420 nm, l = 1 cm.

Variable	Yield of TBO, % from kerogen	Maximum optical density		Rate coefficient, min^{-1}	
		E_{1max} Eq. (23)	E_{2max} Eq. (23)	k_1 Eq. (24)	k_2, Eq. (21)
Pyrolysis nominal temperature 350 °C					
Pyrolysis duration, h					
5	21.4	0.271	–	10.25	–
5.5	53.6	0.652	0.021	0.591	0.021
6	65.7	0.765	0.074	0.625	0.022
7	69.7	0.796	0.059	0.705	0.036
8	83.8	1.049	–	1.109	–
Pyrolysis nominal temperature 360 °C					
Pyrolysis duration, h					
3.5	67.8	0.803	0.053	0.539	0.0517
4	76.8	0.917	0.095	0.686	0.0306
5	80.7	1.023	–	1.208	–
7	83.2	1.038	–	1.164	–
Dissolution temperature, °C					
25	67.4	0.640	0.216	0.133	0.0060
40	67.4	0.743	0.112	0.205	0.0292
60	67.8	0.803	0.053	0.539	0.0517
Pyrolysis nominal temperature 370 °C					
Pyrolysis duration, h					
3	55.1	0.652	0.0506	0.395	0.0481
3.5	80.54	1.021	–	2.257	–
4	81.4	1.032	–	3.175	–
5	83.8	1.062	–	4.096	–

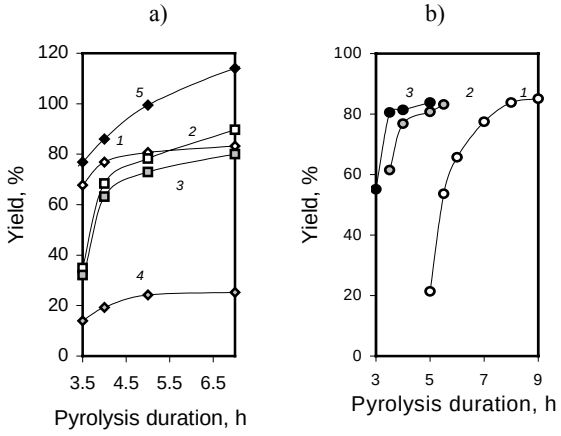

Fig. 1. Effect of pyrolysis duration on the total yield of TBO from kerogen, %, (*a*) solvent type: 1 – benzene, 2 –toluene, 3 – oil shale petrol, 4 – ethanol, 5 – benzene + ethanol; (*b*) pyrolysis nominal temperature: 1 – 350, 2 – 360, 3 – 370 °C.

The default conditions: pyrolysis nominal temperature 360 °C; pyrolysis duration 3.5 h; solvent volume 100 cm^3/g; dissolution temperature 60 °C, solvent – benzene.

Table. 3. **Characteristic constants for TBO dissolution in different solvents**

The default conditions: pyrolysis nominal temperature 360 °C; pyrolysis duration 3.5 h; solvent volume per kukersite 100 cm^3/g; dissolution temperature – 60 °C; dilution factor of the solutions before estimation of their optical density – 10; wave length – 420 nm, l = 1 cm.

Variable	Yield of TBO, % from kerogen	Maximum optical density		Rate coefficient, min^{-1}	
		E_{1max} Eq. (23)	E_{2max} Eq. (23)	k_1 Eq. (24)	k_2 Eq. (21)
Toluene					
Pyrolysis duration, h					
3.5	34.9	0.353	0.054	0.486	0.058
4	68.4	0.822	0.050	0.892	0.035
5	78.3	0.838	0.153	0.960	0.400
7	89.7	1.137	–	2.460	–
Ethanol					
Pyrolysis duration, h					
3.5	13.9	0.086	0.091	0.0632	0.0025
5	24.3	0.202	0.106	0.157	0.0189
7	25.2	0.249	0.070	0.597	0.0402
Solvent volume, cm3/g					
75	15.8	0.057	0.118	0.171	0.0161
100	13.9	0.086	0.091	0.0632	0.0025
150	13.9	0.055	0.101	0.065	0.0016
Oil shale petrol, d = 0.780 g^3/cm^3					
Pyrolysis duration, h					
3	30.8	0.391	–	0.246	–
3.5	32.1	0.407	–	0.322	–
4	63.3	0.802	–	0.983	–
8	83.0	1.052	–	1.998	–
Ethanol + benzene, $(1:1)_V$					
Pyrolysis duration, h					
3	69.5	0.801	0.078	0.763	0.159
3.5	76.9	0.915	0.078	0.544	0.047
5	91.6	1.261	–	0.983	–
8	116.0	1.471	–	1.261	–

Dissolution

The pyrolyzed sample stuck, as a rule, in the form of the stick-like inner volume of the glass test-tube. Dissolution of the product with any solvent in a flow tube-reactor without stirring failed revealing that an active agitation of the suspension was required. For this aim, in the next experiments the pyrolyzed sample was quantitatively poured into 100 cm^3 thermostated (20-60 °C) dissolution solvent in a refluxed flask stirred with an anchor mixer with constant rotation rate, 3000 turns/min. After certain intervals a volume V_{an} was taken from the solution for photometric determination of optical density (E*) of the solutions by a spectrophotometer SPEKOL 11. As far the solution volume per mass of the sample decreased with every volume taken

for the analysis, the corrected current optical densities (E_n) were calculated as follows:

$$E_n = \left\{ \sum_{i=1}^{n-1} E^*_i V_{an} + E^*_n \left[V - (n-1) V_{an} \right] \right\} / V. \quad (6)$$

The plot of optical density at the wave length 420 nm *versus* TBO concentration estimated by weight has given a linear calibration graph with slope 3.21 $dm^3(cm\ g)^{-1}$. So, the current yield of TBO at dissolution from its total soluble quantity in the solvent, C/C_{max}, should be equal with the ratio of the corresponding optical densities, E/E_{max}.

The experimental results prove the modeled earlier regularities [4] – the yield of TBO increases with pyrolysis time and temperature (Fig. 2a). Besides, as it can be expected, the rate increases with dissolution temperature (Fig. 2b). But the effects of the solvent volume (Fig. 2c) and type (Fig. 2d) are insignificant, except ethanol whose dissolution possibility is remarkably lower.

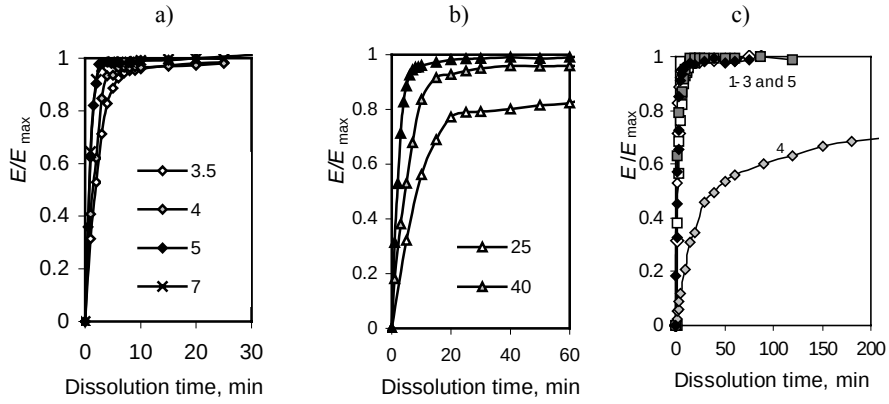

Fig. 2. Effect of dissolution time on the dissolution degree of TBO formed at different variables: (*a*) pyrolysis duration, h; (*b*) dissolution temperature, °C; (*c*) solvent type (see the symbols in Fig. 1a).

The default conditions see in Fig. 1.

TBO dissolution kinetics

Suitability of the known dissolution models

For quantitative comparison of the effect of various solvents on the TBO dissolution kinetics, the rate coefficient k was estimated by different kinetic models. Fitness of the models was evaluated by invariability of their k during dissolution. For this aim, linearity between $g(x)$ and t according to Eq. (5) was tested using the models given in Table 1 for calculation of $g(x)$.

At first, the typical dissolution model described by Eq. (3) was tested. For estimation of the two unknown constants, E_S and k, the equation was written as

$$k = \frac{\ln\left(1 - \frac{E}{E_S}\right)}{t}, \tag{7}$$

and the least squares method was applied introducing the series of experimentally found E and t values. At that, for the most of the dissolution conditions studied the best fit of k was obtained at a value of E_S proposed that provided unacceptable systematically decreasing in time values of k with a high (10–30%) mean dispersion. So, the model with diffusion layer concentration does not agree with experimental results.

In the following calculations, considering the exhaustible amount of TBO, the dissolution degree, $x = E/E_{max}$ was used where the maximum value of optical density was found experimentally as the mean during 2–3 hours dissolution.

Unsuitability of the "Power law" model, Eq. (4), was proved by curvilinear shape of the logarithmic relationship between x and t.

The plots of $g(x)$ calculated according to the formulas given in Table 1 *versus* dissolution time for the default conditions given in Tables 2 and 3 are presented in Fig. 3a. At that, the values of $g(x)$ in Fig. 3a are normalized by dividing with their values at 30 min., and in 3b with those at 10 min. The curves obtained evidence that Models *I* and *III–X* give quite similar convex-type curves suggesting decreasing in time rate coefficients, and Model II (n = 2, 3, and 4) oppositely, concave-type ones. But there are some experi-

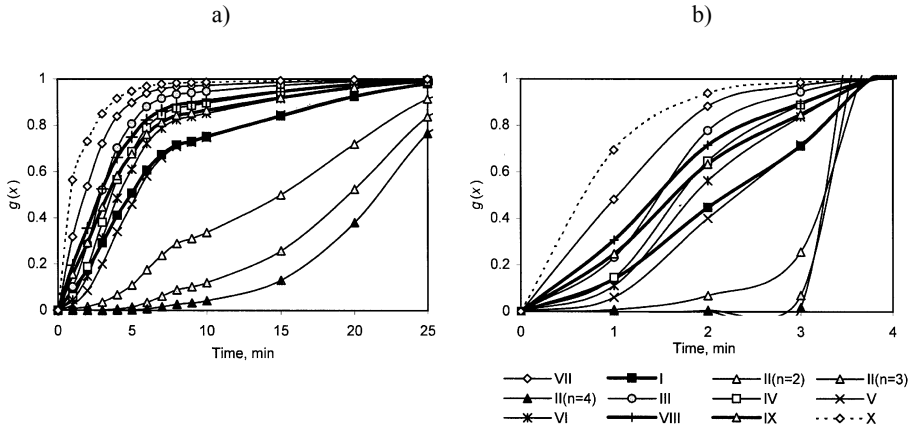

Fig. 3. Effect of dissolution time on the current values of $g(x)$ calculated by different models: (*a*) for the default conditions, (*b*) for pyrolysis temperature 370 °C and time 3.5 h. The numbers of curves are equivalent with their formula numbers in Table 1.

The default conditions see in Fig. 1.

mental conditions whose results can be approximated to a linear relationship, particularly following the first order kinetic model I, (Fig. 3b, curve *I*). These phenomena will be discussed later below.

Model for the two-stage parallel dissolution

For more adequate modeling of TBO dissolution kinetics, all the curves in Fig. 3a can be more or less satisfactorily approximated to two intersecting straight lines belonging to two stages. The first stage is compiled from parallel dissolution of two fractions with different dissolution rate coefficients. As soon as dissolution of the first component has reached its steady state, the next stage begins where dissolution of the single second component takes place. Basing on Fig. 3b, the first order Model *I* has been chosen from the bulk of formulas *I–X*.

The two straight lines are expressed by the following formulas:

$$Y_1 = b_1 t \tag{8}$$

and

$$Y_2 = a_2 + b_2 t \tag{9}$$

having their intersection point at time

$$t' = a_2/(b_1 - b_2). \tag{10}$$

Admitting that in the first stage the parallel dissolution of the lower-molecular weight fraction (1) and higher-molecular weight fraction (2) takes place, an increase in the total optical density of the solution should follow the relationship

$$\mathrm{d}E/\mathrm{d}t = k_1(E_{1\max} - E_1) + k_2(E_{2\max} - \mathrm{E}_2), \tag{11}$$

where the rate coefficients k_1 and k_2, and the maximum optical densities $E_{1\max}$ and $E_{2\max}$ are four unknown constants to be estimated. Besides, the current optical densities of the two components (E_1 and E_2) having coinciding spectra cannot be measured separately either. The experimentally recorded values are their sums

$$E_{\max} = E_{1\max} + E_{2\max} \tag{12}$$

and

$$E = E_1 + E_2. \tag{13}$$

Algorithm for estimation of k_2

For estimation of the unknown constants, the second stage beginning from t' determined by Eq. (10) is handled at first. As far during this stage the current and maximum total optical densities differ from those of the second component by $E_{1\max}$, the following equalities are valid:

$$dE/dt = k_2(E_{max} - E), \quad (14)$$

$$dE_2/dt = k_2(E_{2max} - E_2). \quad (15)$$

Integration of Eq. (14) in the boundaries from E' to E and t' to t gives

$$\ln\frac{1-\frac{E'}{E_{max}}}{1-\frac{E}{E_{max}}} = k_2(t-t'). \quad (16)$$

Eq. (16) can be presented in the form of a linear regression

$$y = A_2 + B_2x, \quad (17)$$

where

$$y = \ln\left(1-\frac{E}{E_{max}}\right), \quad (18)$$

$$x = (t - t'), \quad (19)$$

and the regression coefficients

$$A_2 = \ln\left(1-\frac{E'}{E_{max}}\right), \quad (20)$$

$$B_2 = -k_2. \quad (21)$$

Algorithm for estimation of E_{1max} and E_{2max}

The integrated form of Eq (11) describes the time-dependence of the total optical density

$$E = E_{1max}[1 - \exp(-k_1t)] + E_{2max}[1 - \exp(-k_2t)]. \quad (22)$$

In the second stage where dissolution of the first component is completed

$$E = E_{1max} + E_{2max}[1 - \exp(-k_2t)]. \quad (23)$$

Eq. (23) should express a straight line of the current optical densities versus the current shares of not dissolved second component expressed as $[1 - \exp(-k_2t)]$. So, the regression constants in Eq. (23) correspond directly to the maximum optical densities of the components.

Algorithm for estimation of k_1

The value of k_1 can be found as a slope of the linear regression obtained after replacements in Eq. (22) as follows:

$$Y = -\ln\{1 - [E - E_{2max}(1 - \exp(-k_2t)]/E_{1max}\} = k_1t \quad (24)$$

introducing the constants k_2, E_{1max} and E_{2max} found as described above and the current optical densities in the first stage where $t < t'$.

The values of k_2, E_{1max}, E_{2max} and k_1 and found by Eqs. (16), (21), (23) and (24) are gathered in Tables 2 and 3.

Algorithm for estimation of current dissolution yields

The current concentration of TBO in the dissolution solutions is calculated as

$$C = \frac{EV}{BV_{an}l}, \tag{25}$$

where V/V_{an} is the dilution degree of the solution for analysis, B is the special absorptivity of TBO equal to the slope of the calibration curve at the wavelength applied, and l is the length of the optical path.

The current yield of TBO from the sample being dissolved, in grams per 100 gram of the initial organic matter (kerogen)

$$\alpha_{OM} = 100CV/G, \tag{26}$$

where V is volume of the dissolution solution (dm^3), and G is mass of the initial sample or its kerogen at the low-temperature pyrolysis.

Results and discussion

Estimation of the dissolution rate coefficients and maximum optical densities

The values of E estimated in every series were introduced into the first order kinetic formula I given in Table 1 and plotted against the corresponding dissolution time. As examples, the curves for dissolution of TBO in benzene at 360 and 370 °C are presented in Fig. 4a. The distinct difference between the two stages evident for 360 °C (curves 1–3) allows estimation of the regression coefficients b_1, a_2 and b_2 according to Eqs. (8) and (9). For 370 °C (curve 4) a linear relationship is kept up to the function value –4.3 corresponding to the dissolution degree 0.986 from the total soluble TBO. So, the single stage model can be applied for description of the dissolution process under the last conditions, and similar ones. In such cases the slope is equivalent to the single dissolution rate coefficient $-k$.

According to Eq. (21), the value of $-B_2$ for the second stage is equal to k_2. All the second stage rate coefficients for the two-stage processes revealed under the conditions studied are given in the last columns of Tables 2 and 3. In conditions where the one-stage mechanism describes the kinetics satisfactorily, the values of k_2 are absent in the columns.

For estimation of E_{1max} and E_{2max}, the current optical densities estimated in the second stage were plotted against the function $1 - \exp(-k_2 t)$ according

to Eq. (23). Some examples are given in Fig. 4b. The values of the maximum optical densities found from the slope and intercept are presented in the third and fourth columns of Tables 2 and 3.

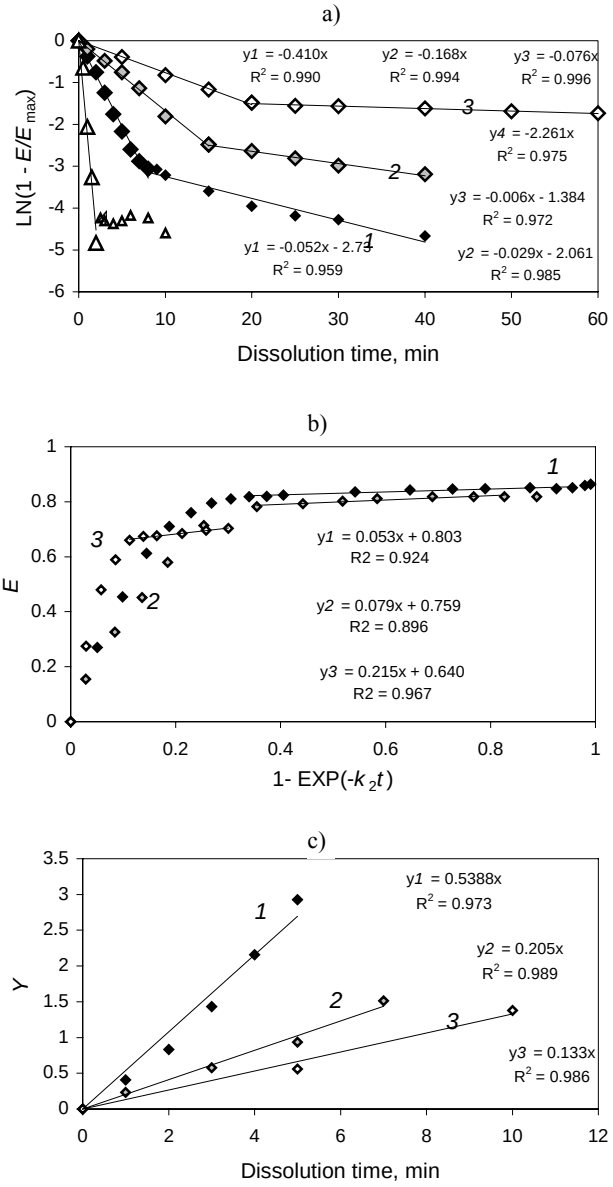

Fig. 4. Plot of the assisting functions for calculation of the constants: (*a*) k_2 by Eq. (14, 19); (*b*) E_{1max} and E_{2max} by Eq. (21); (*c*) k_1 by Eq. (22) for dissolution temperatures: 1 – 60; 2 – 40 and 3 – 25 °C, and 4 in Fig. (*a*) – for pyrolysis temperature 370 °C.

The default conditions see in Fig. 1.

At last, the values of k_1 were estimated as the slope introducing the values of t and E of the first stage into Eq. (24). Some examples are depicted in Fig. 4c. The values found are given in the fifth column of Tables 2 and 3.

The data obtained (Tables 2 and 3) evidence that, as a rule, the dissolution kinetics characterized by a single stage and rate coefficient is appropriate in conditions resulting in higher (over 80%) decomposition degree of oil shale organic matter, for example at prolonged pyrolysis durations or at higher pyrolysis temperatures. On the contrary, the one-stage dissolution scheme can be applied also at the beginning of thermal decomposition (below 25%) at 350 °C. Noteworthy is that, despite the low yield, the dissolution process of TBO in ethanol consists of two stages, and the dissolution in oil shale petrol is an one-stage process at any pyrolysis duration and corresponding yield of TBO obtained.

Prediction of the current optical densities of the dissolution solutions

When the values of k_1, k_2, E_{1max} and E_{2max} have been estimated, the current values of optical density over the both stage can be predicted by Eq. (22). As examples, the plots of E versus t are depicted in Fig. 5 for the two-stage dissolution scheme of TBO obtained by pyrolysis at 360 °C under the three dissolution temperatures 25, 40 and 60 °C (curves 1–3), and an one-stage process under temperature 60 °C of TBO obtained at 370 °C (curve 4).

The current concentration and yield of TBO can be calculated according to Eqs. (25) and (26).

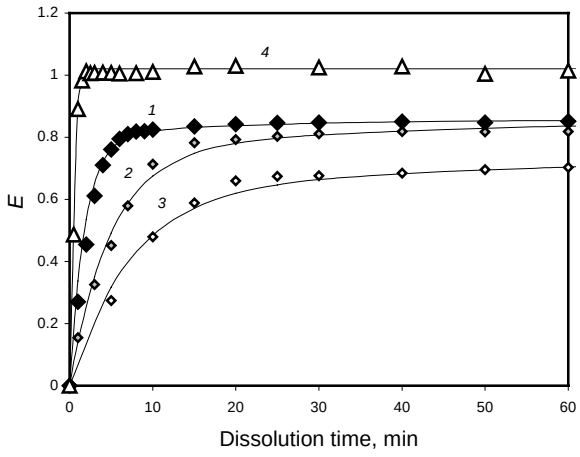

Fig. 5. Plot of optical density versus dissolution time for dissolution temperatures, °C: 1 – 60, 2 – 40, 3 – 25, and 4 – for pyrolysis temperature 370 °C.

Points experimental, curves – calculated.

Dilution factor of the solutions before estimation of their optical density – 10; wave length – 420 nm, l = 1 cm. The default conditions see in Fig. 1.

Conclusions

Dissolution kinetics of the mix of thermobitumen and oil (TBO) obtained at low-temperature pyrolysis of kukersite in various solvents was studied for the first time. The main results of the study were as follows:

- Dissolution of the sticky TBO needs an active stirring and allows under optimal conditions separation of 80–90% from the kukersite organic matter as a liquid product.
- The yield of TBO into the solvents applied increases in the row: ethanol << oil shale petrol ≈ benzene < toluene < benzene + ethanol whereas part of ethanol incorporates into TBO.
- The dissolution of TBO at an active stirring is faster (less than 30 min) than formation of TBO (3.5–5 hours) and depends mainly on the decomposition degree of the initial kerogen determined by the pyrolysis temperature and duration, and on the dissolution temperature. The effect of solvent type on the dissolution rate is negligible, except in ethanol.
- The dissolution kinetics under the conditions enabling low (below 25%) and high (over 80%) total yield of TBO can be described by the first-order kinetic model, except in ethanol. Under conditions enabling the total yield of TBO in the range of 25–80%, and in ethanol at any yield, the fourteen known kinetic models tested were unsuitable for description of the process.
- A mathematical model basing on the scheme of parallel first-order dissolution of two fractions has been deduced for satisfactory description of the dissolution kinetics of TBO not fitting under the models known earlier.
- The rate coefficients for dissolution of the fractions, and the maximum optical densities of their solutions were estimated for the conditions studied.

Acknowledgements

The authors thank Estonian Science Foundation for the financial support by Grant No. 7292 and Estonian Ministry of Education and Research for financiering SF014002809.

REFERENCES

1. *Aarna, A. Y., Lippmaa, E. T.* Thermal destruction of oil shale-kukersite // Trans. Tallinn Polytechnic Institute. Series A. 1958. No. 97. P. 3–27 [in Russian].

2. *Zaidentsal', A. L., Soone, J. H., Muoni, R. T.* Yields and properties of thermal bitumen obtained from combustible shale // Solid Fuel Chemistry. 2008. Vol. 42, No. 2. P. 74–79.
3. *Tiikma, L., Zaidentsal, A., Tensorer, M.* Formation of thermobitumen from oil shale by low temperature pyrolysis in an autoclave // Oil Shale. 2007. Vol. 24, No 4. P. 535–546.
4. *Johannes, I., Tiikma, L., Zaidentsal, A., Luik, L.* Kinetics of kukersite low-temperature pyrolysis in autoclaves // J. Anal. Appl. Pyrolysis. 2009. Vol. 85, No. 1–2. P. 508–513.
5. *Johannes, I., Zaidentsal, A.* Kinetics of low-temperature retorting of kukersite oil shale // Oil Shale. 2008. Vol. 25, No 4. P. 412–425.
6. *Tiikma, L., Johannes, I., Luik, H., Zaidentsal, A., Vink, N.* Thermal dissolution of Estonian oil shale // J. Anal. Appl. Pyrolys. 2009. Vol. 85, No. 1–2. P. 502–507.
7. *Luik, H., Klesment, I.* Liquefaction of kukersite concentrate at 330-370 °C in supercritical solvents // Oil Shale. 1997. Vol. 14, No. 4. P. 419–432.
8. *Luik, H., Palu, V., Bityukov, M., Luik, L., Kruusement, K., Tamvelius, H., Pryadka, N.* Liquefaction of Estonian kukersite oil shale kerogen with selected superheated solvents in static conditions // Oil Shale. 2005. Vol. 22, No. 1 P. 25–36.
9. *Dokoumetzidis, A., Macheras, P.* A century of dissolution research: From Noyes and Whitney to the biopharmaceutics classification system // Int. J. Pharm. 2006. Vol. 321, No. 1–2. P. 1–11.
10. *Noyes, A., Whitney, W. R.* The rate of solution of solid substances in their own solutions // J. Am. Chem. Soc. 1897. Vol. 19, No. 12. P. 930–934.
11. *Nernst, W.* Theorie der Reaktionsgeschwindigkeit in heterogenen Systemen // Z. Phys. Chem. 1904. Vol. 47. P. 52–55.
12. *Skrdla, P. J.* A simple model for complex dissolution kinetics: A case study of norfloxacin // J. Pharm. Biomed. Anal. 2007. Vol. 45, No. 2. P. 251–256.
13. *Peppas, N. A.* Analysis of Fickian and non-Fickian drugrelease from polymers // Pharm. Acta Helv. 1985. Vol. 60, No. 4. P. 110–111.
14. *Galwey, A. K., Brown, M. E.* Thermal Decomposition of Ionic Solids: Chemical Properties and Reactivities of Ionic Crystalline Phases, 1st ed. – Elsevier, Amsterdam, 1999. P. 75.
15. *Khawam, A., Flanagan, D. R.* Role of isoconversional methods in varying activation energies of solid-state kinetics. I. Isothermal kinetic studies // Thermochim. Acta. 2005. Vol. 429, No. 1. P. 93–102.
16. *Khawam, A., Flanagan, D. R.* Role of isoconversional methods in varying activation energies of solid-state kinetics. II. Nonisothermal kinetic studies // Thermochim. Acta. 2005. Vol. 436, No. 1–2. P. 101–112.
17. *Skrdla, P. J., Robertson, R. T.* Dispersive kinetic model for isothermal solid state conversions and their application to the thermal decomposition of oxacillin // Thermochim. Acta. 2007. Vol. 453, No. 1. P. 15–20.
18. *Aboulkas, A., El Harfi, K., El Bouadili, A., Benchanaa, M., Mokhlisse, A., Outzourit, A.* Kinetics of co-pyrolysis of Tarfaya (Morocco) oil shale with high-density polyethylene // Oil Shale. 2007. Vol. 24, No. 1. P. 14–33.
19. *Aboulkas, A., El harfi, K., El bouadili, A.* Kinetics and mechanism of Tarfaya (Morocco) and LDPE mixture pyrolysis // J. Mat. Proc. Technol. 2008. Vol. 206, No. 1–3. P. 16–24.

20. *Yang Xulai, Zhang Jian, Zhu Xifeng*. Thermal degradation kinetics of calcium-enriched bio-oil // AIChE J. 2008. Vol. 54, No. 7. P. 1945–1950.
21. *Farjas, J., Roura, P.* Simple approximate analytical solution for nonisothermal single-step transformations: kinetic analysis // AIChE J. 2008. Vol. 54, No. 8. P. 2145–2154.
22. *Ortega, A.* A simple and precise linear method for isoconversional data // Thermochim. Acta. 2008. Vol. 474, No. 1–2. P. 81–86.
23. *Öpik, I., Golubev, N., Kaidalov, A., Kann, J., Elenurm, A.* Current status of oil shale processing in solid heat carrier UTT (Galoter) retorts in Estonia // Oil Shale. 2001. Vol. 18, No. 2. P. 99–108.

Presented by A. Kogerman
Received January 20, 2009